WPPMI-CPR(18) 19371

M Siccinio et al.

Development of a plasma scenario for the EU-DEMO: current activities and perspectives

Preprint of Paper to be submitted for publication in Proceeding of
27th IAEA Fusion Energy Conference

This work has been carried out within the framework of the EUROfusion Consortium and has received funding from the Euratom research and training programme 2014-2018 under grant agreement No 633053. The views and opinions expressed herein do not necessarily reflect those of the European Commission.

Development of a plasma scenario for the EU-DEMO: current activities and perspectives

M. Siccinio[1,2*], E. Fable[2], F. Janky[2], R. Ambrosino[3], W. Biel[4], M. Cavedon[2], Th. Franke[1,2], G. Granucci[5], Th. Härtl[1,2], V. Hauer[6] I. Ivanova-Stanik[7], R. Kembleton[1,8], Y.Q. Liu[9], H. Lux[8], M. Mattei[10], F. Maviglia[1,3], J. Morris[8], F. Palermo[2], G. Pautasso[2], L. Pigatto[11], E. Poli[2], S. Saarelma[8], O. Sauter[12], F. Subba[13], M. Q. Tran[12], E. Viezzer[14], P. Vincenzi[11], Ch. Vorpahl[1,6], L.N. Zhou[15], H. Zohm[2]

[1]EUROfusion Consortium, Garching bei München, Germany - [2]Max-Planck-Institut für Plasmaphysik, Garching bei München, Germany
[3]Consorzio CREATE, Università di Napoli Federico II, Napoli, Italy - [4]Forschungszentrum Jülich, Jülich, Germany
[5]Istituto Nazionale di Fisica del Plasma, Milano, Italy -[6] Karlsruhe Institut für Technologie (KIT), Karlsuhe, Germany
[7]Institute of Plasma Physics and Laser Microfusion, Warsaw, Poland
[8]Culham Centre for Fusion Energy, Abingdon, United Kingdom - [9]General Atomics, San Diego, USA
[10]Consorzio CREATE, Università della Campania "Luigi Vanvitelli", Napoli, Italy - [11]Consorzio RFX, Padova, Italy
[12]École Polytechnique Fédérale de Lausanne, Swiss Plasma Center, Lausanne, Switzerland - [13]NEMO group, Politecnico di Torino, Torino, Italy
[14]Universidad de Sevilla, Sevilla, Spain - [15]Dalian University of Technology, Dalian, People Republic of China

*Corresponding author. Tel.: +49 (0)89-3299-1843. E-mail address: mattia.siccinio@euro-fusion.org

Abstract

In order for the first fusion reactor DEMO to accomplish its mission, it is necessary to identify plasma scenarios which both perform in terms of fusion power generation and are sufficiently stable to ensure the integrity and availability of the machine components for a long time. This means, in particular, considering from the early phases their compatibility with the available diagnostics, with the suitable actuators for plasma control and with the power limitations of the heating and current drive (H&CD) systems. The activities undertaken for this purpose inside the EUROfusion Power Plant Physics & Technology division (PPP&T) are summarized in this paper. A coupling between the 1D transport code ASTRA and the control software Simulink has been performed, providing a tool capable of simulating plasma behaviour while accounting for the constraints linked to the detectability of the signals and the delay and power limitations of the actuators responses. Here, some DEMO related results of such tool are presented. In parallel, the numerous ongoing activities concerning the open issues which require addressing are reviewed. The reference scenario which is considered for the EU-DEMO is the so called "DEMO 1", i.e. a pulsed configuration based on conservative physics assumptions and, at least from a macroscopic level, up-scaled from the ITER 15 MA ELMy-H mode. The main alternative concept developed is the so called Flexi-DEMO, which relies on a more advanced scenario compared to DEMO 1, with a large fraction of auxiliary current drive and a tailoring of the safety factor profile, in order to maximize the bootstrap current fraction and thus to achieve a long, or even steady-state discharge. However, the significant difficulties linked to an active ELM control suggest that other, more speculative ELM-free scenarios might be better suitable for a reactor operation – in spite of their reduced fusion performance, or their challenging accessibility.

Introduction

With the expression "plasma scenario" it is indicated a self-consistent description of the kinetic profiles and of the magnetic equilibrium during the flat-top of the plasma discharge, as well as during the transients to access it (ramp-up) and to terminate it (ramp-down or emergency termination). Furthermore, such expression encompasses a determination of the necessary diagnostic and actuator performance for plasma control (e.g. H&CD power and deposition profiles, fuel injection rate and pumping rate, magnetic fields for plasma shaping and position control), the verification of the plasma stability both in flat-top and during the transients and the assessment of the corresponding divertor heat loads associated to the chosen operational point in the various phases of the discharge. Finally, the description of the plasma scenario must include an assessment of the consequences of unplanned incidental transients, as well as the countermeasures to the associated risks, e.g. a plasma-wall contact. The mission of the prototypical fusion reactor DEMO is to demonstrate nuclear fusion to be a technologically reliable source for the production of electrical energy [1]. This requires the identification of plasma scenarios which are at the same able to provide a sufficient amount of fusion power and to ensure the integrity and availability of the machine components for a long time. This leads to the following high-level plasma scenario criteria:

- Providing a sufficient amount of fusion power so to ensure a sufficient electric power output. This translates in possessing a high plasma confinement capability and in avoiding the accumulation of impurities in the plasma core, both seeded and intrinsic. Preliminary investigations with the transport code ASTRA [2,3,4] have shown that, in order to achieve the design target fusion power of 2 GW while maintaining β_N below the relevant stability limits, and assuming a H_{98} factor around 1.0, a machine of approximatively 9 m major radius is required. Also, the same simulations have pointed out that a maximal He concentration of about 7.5% in the centre appears to be compatible with the reactor operation.

- Requiring a sufficiently low auxiliary recirculated H&CD power during flattop in comparison to the expected electricity generation. Calculations performed with the systems code PROCESS [5,6] show that, to deliver a net electrical output of around 500 MW at the mentioned fusion power level of 2 GW, the time-averaged H&CD power requirement during the flat-top phase must remain at a few tens of MW launched to the plasma in average, while for short periods it can be larger.

- Being disruption-free or as stable as possible against disruptions, both during the flattop and during the transients, planned and unplanned, since every disruption is expected to cause an interruption of the plant operation for inspection or even repair. Although a precise determination of the maximum tolerable disruption rate is still under investigation, it is assumed that a fusion power plant cannot be attractive with more than one disruptive event (even mitigated, since the stored energy in DEMO is much higher compared to present days experiments) every two full-power years, or less. It is however important to stress that the disruption avoidance has to be understood as a control aim, and not as a problem of plasma physics alone.

- Maintaining, also in absence of disruptions, the heat load on the plasma facing components below the prescribed technological limits during all relevant plasma phases, with particular attention to the off-normal events such like accidental divertor plasma reattachment.

- Finally, the plasma scenario should be capable of being tested in ITER, and/or on other future devices with dominant alpha heating. In general, DEMO is not conceived as a physics experiment, but as a machine with stringent availability requirements. That is, the plasma scenario should be well-understood under relevant condition before being deployed in DEMO.

Various activities concerning the physics gaps of DEMO have been undertaken in the last years in the EUROfusion Power Plant Physics and Technology (PPP&T) department, addressing both the peculiar aspects of plasma physics as well as the integration with the relevant engineering aspects [7,8]. In the present work, the current status of these activities is presented and reviewed.

The reference scenario which is considered for the EU-DEMO is the so called “DEMO 1” [9], i.e. a pulsed scenario with about 18 MA of plasma current, not relying on auxiliary bulk current drive from the plasma heating systems during the flat-top phase. DEMO 1 targets at 2 GW of fusion power outcome and a pulse length of 2 hours, with a duty cycle pulse/dwell of 12 (7200 s/600 s), based on prudential physics assumptions and analogous, at least from a macroscopic level, to the ITER 15 MA baseline scenario. This represents in some sense the most natural choice for the first electricity producing fusion reactor, for the simple reason that, in the future, such a scenario is expected to be supported by the experimental results of the ITER burning plasmas, which are an essential step towards the realization of fusion power plants. However, other, alternative scenarios are investigated in parallel.

The main alternative concept developed is the so-called Flexi-DEMO scenario, which has been conceived as the intermediate step between ITER and future fusion power plants in the “stepladder” approach [10]. Flexi-DEMO relies on more advanced scenarios as compared to DEMO 1, with a large fraction of auxiliary current drive and a tailoring of the safety factor profile which aims at maximizing the bootstrap current fraction – to some extent analogous to the ITER 9 MA scenario. The idea behind Flexi-DEMO is to absorb all the uncertainties connected to the achievable energy confinement and plasma stability limits by adjusting the discharge duration (to a level which is compatible with the capability of the engineering systems to handle pulsed loads), ensuring however the fusion power outcome in order to avoid significant repercussions on the balance of plant and on the breeding blanket performance. At sufficiently high confinement, a steady state operation becomes possible. From the point of view of the scenario integration, the main difficulty of Flexi-DEMO is linked to the constant necessity of a high and efficient auxiliary current drive, which must be added on top of the other functions of the auxiliaries, as, for example, the control of the instabilities. Also, at higher confinement and β_N, Flexi-DEMO is prone to Resistive Wall Modes (RWMs), needing therefore active Resonant Magnetic Perturbations (RMP) control coils, whose performance requirements are currently under investigation.

During the currently ongoing pre-conceptual design phase it clearly emerged the necessity of considering from the early phases the compatibility of the plasma scenarios with the performance of the available diagnostics, actuators for plasma control and with the power limits of the heating and current drive systems. For this reason, a coupling between the 1D transport code ASTRA and the control software Simulink has been performed, providing a tool able to simulate the plasma behaviour while accounting for the limitations linked to the detectability of the signals, thus assuming realistic diagnostic properties, and considering the delays and the power limitations of the actuators responses as well [11]. In the present paper, some of the DEMO-related results of such a tool are presented. Long term goal is to further develop this tool, allowing the identification of criticalities in the diagnostics and control system in a broad sense, in particular for those chains of events which can lead to a plasma disruption. First test runs have been performed, the results being discussed under section 2.

In addition, various activities concerning the physics gaps of DEMO have been undertaken. In the present work we focus in particular on the following aspects:

- Sawteeth (and NTM) control strategy
- Integrated core/pedestal predictive modelling
- SOLPS divertor simulation, also in support of
- Development of synthetic diagnostics for divertor detachment
- Assessment of the pumping requirements
- Ramp up and down modelling
- Edge Localised Modes (ELMs) and ELM-free regimes [12,13]

Finally, also the latest investigations on Flexi-DEMO – mostly focused on the configuration peculiarities, i.e. the evaluation of the current drive efficiency are presented. In contrast, the analysis of the consequences of disruptions, as well as their mitigation strategy, is left outside from this paper and will be reported in separated publications.

1. DEMO 1 Baseline

In spring 2018, a new physics baseline for EU-DEMO 1 produced by means of the systems code PROCESS [5,6] has been released. The requirements of 2000 MW fusion power, 500 MW plant net electric output power as well as the 2 hours burn time have been maintained the same as in the 2017 baseline. Table 1 summarizes the most relevant (physics related) parameters of EU-DEMO 2018 for the Flat Top (FT) plasma phase. The corresponding values of 2017 baseline are also reported for comparison.

	DEMO Physics 2018	DEMO Baseline 2017
R [m]	9.00	8.93
B_0 [T]	5.86	4.89
q_{95}	3.89	3
I_p [MA]	17.75	19.07
P_{fus} [MW]	2000	2000
P_{sep} [MW]	170.4	156.4
P_{aux} [MW]	50	50
$H^*_{rad,corr}$	1.1	1.1
H_{98}	0.98	0.99
$< n > / n_{GW}$	1.2	1.2
$< T >$ [keV]	12.49	12.82

***Table 1**. DEMO 1 relevant machine parameters according to the Physics Baseline 2018 and corresponding parameters for the 2017 Baseline. Data have been produced with the systems code PROCESS.*

As one can observe, the main modifications with respect to the previous baseline are:

- Stronger magnetic field by maintaining (almost) the same major radius. This has been made possible by the improvement of the calculation method for the effective plasma charge Z_{eff} which has led to a reduction of the size of the central solenoid, enabling a larger TF coil.
- Larger safety factor at the edge. This makes the plasma configuration more robust against disruptions.
- Larger power crossing the separatrix. The employed figure of merit $P_{sep}B/q_{95}AR$ for the divertor compatibility benefits of the larger safety factor, in turn reflecting a larger power decay length λ_q as a consequence of the widely employed Eich scaling [14,15].

The value of the auxiliary power $P_{aux} = 50$ MW represents an average for the necessary control power during the flat-top (e.g. for MHD control or for burn control), which in reality is not constant in time but can vary in accordance to the plasma control requirements. For DEMO 1, no explicit need for a plasma bulk current drive (CD) is foreseen. Also, no final decision has been currently taken regarding which H&CD technology (EC, NB, or IC) is charged of each H&CD function.

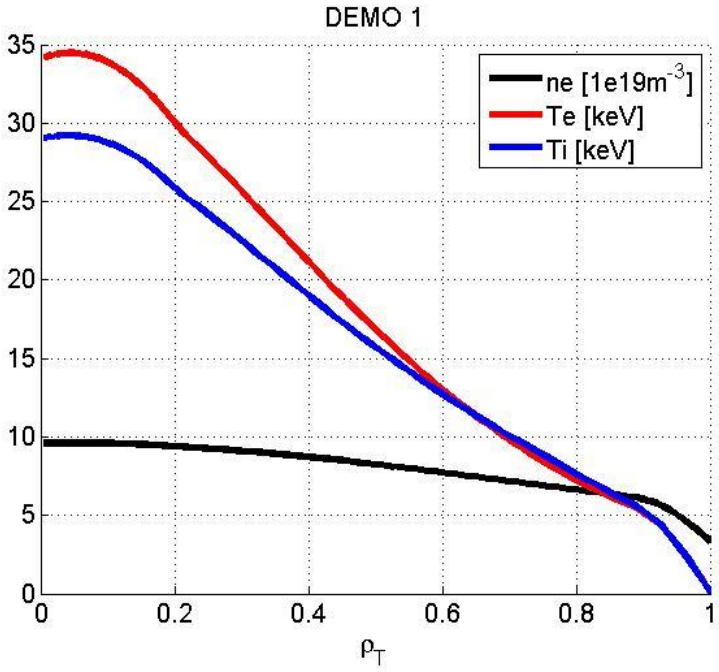

***Figure 1**. Density and temperature profiles for DEMO 1 Physics Baseline 2018 calculated with ASTRA. Those profiles are then used as a basis for subsequent investigations – e.g. for sawteeth stability analysis (see below).*

Density and temperature profiles of the 2018 DEMO baseline, calculated with ASTRA, are visualized in Fig. 1. The reference DEMO 1 scenario is analogous to the ITER 15 MA baseline scenario, both assuming a pulsed operation with a confinement time in line with what foreseen by the well-known IPB98(y,2) scaling. There are however some aspects on which the two scenarios have to differ, for reasons essentially linked to the different missions of ITER and DEMO, as for example the large amount of core radiation which is necessary in DEMO to reduce the divertor challenge [7]. The presence of a core radiator, like for example Xe, has significant impact on the plasma control, in view of the large residence time foreseen for such species in the confined plasma, as discussed in the next section.

2. ASTRA/Simulink coupling

As mentioned in the introduction, one of the main targets for the plasma scenario development in the current pre-conceptual design analysis phase for the European DEMO is to address the scenario compatibility with the performance of the available diagnostics and actuators. For this reason, a coupling between the 1D transport code ASTRA and the control software Simulink has been performed. The resulting tool is simulating the plasma behavior while accounting for the limitations linked to the detectability of the signals whilst also considering the delays and the power limitations of the actuator responses. The reader interested to the detail of the physics modelling and of the control mechanisms implemented is referred to the dedicated paper [11]. Here, only two examples of the possible use for the plasma scenario definition in DEMO are presented. It is however important to stress that the code is still considered under development, and many fundamental aspect for a real and complete DEMO discharge description are missing. The examples below have thus to be understood as illustrative of the potentiality of the tool, but not as validated DEMO control schemes, nor as realistic discharges. These first results are however quite helpful to highlight the importance of such control tools.

In the first example (Fig. 2), a simultaneous control simulation of the fusion power, of the pedestal top density and of the power crossing the separatrix, aiming at maintaining the DEMO plasma around some given reference values for these quantities (2 GW, $0.9n_{GW}$ and 220 MW, respectively, where n_{GW} is the Greenwald density) is presented. The foreseen actuators for this control target are an auxiliary heating source (NBI – with a maximum allowable power set for the present case to 100 MW), a material injection system – namely a pellet injector, and a xenon injector, where the xenon is employed as a core radiator to prevent an excessively high power at the separatrix. For the pellet injection, different delivery success rates have been considered. In particular, the blue curves in Fig. 2 below refer to a 0% failure rate – i.e. all the pellets are delivered when requested, whereas the green curves refer to a 10% failure rate (more realistic in accordance with present experiments), with the missing pellets being randomly distributed in time. Reference values imposed as a target by the controller are shown in all panels with a thick red line.

For the first 50 seconds, the density at the pedestal top is ramped until the required, reference value is reached (Fig 2. - third panel). During this phase, the NBI is turned on to prevent an excessive decrease in fusion power (second panel). Once the desired fusion power level has been reached, the signal stays very close to the reference value if no pellet failure is considered (first panel). Otherwise, oscillations are significant, although quite slow, and the unavoidable time shift between the pellet failure and the heat deposition from the NBI can even determine an increase of the fusion power beyond the target level. The removal of excess Xe from the system is quite slow, thus the power at the separatrix follows on a much slower timescale. From $t = 200$ sec on, a decrease in the density at the pedestal-top is imposed by the controller, and the simulation attempts to maintain the fusion power at the same level. The actual value of the density follows quite slowly, but clearly the NBI must now compensate to

keep the plasma hot enough. The reference fusion power cannot be reached with such a low pedestal density, even at $t = 400$ sec., where the simulation has then been stopped.

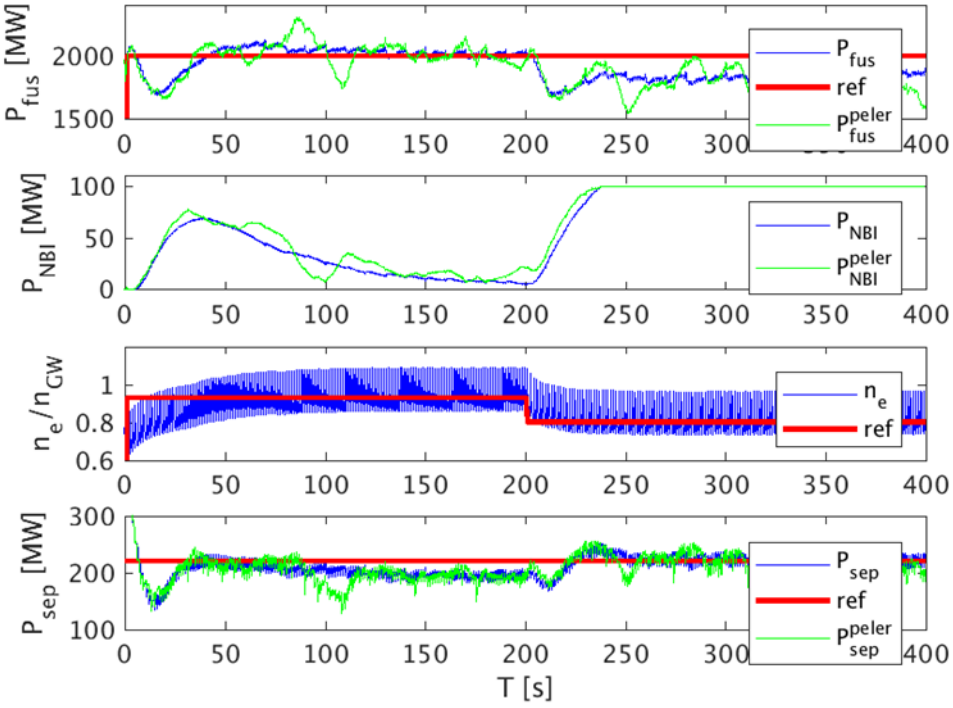

***Figure 2**. Simulation of fusion power control with ASTRA/Simulink in presence of a pellet injection system with a delivery success rate of 100% (blue curves) and 90% (green curves). Target of the present control scheme is to maintain the fusion power, the pedestal top density and the power crossing the separatrix to a target value indicated by the red thick lines. At t = 200 sec, the controller imposes a decrease in the density value at the pedestal top. The figure is discussed in more detail in the main text.*

In the second example (Fig. 3), a fusion power control in presence of a loss of divertor detachment with subsequent W erosion and plasma dilution via impurity influx is presented. The actuators are in this case a Xe injection system, an Ar injection to radiate energy from the SOL/divertor region – and thus to recover the detachment – and again the NBI to compensate for the energy losses induced by the W in the plasma core.

At $t = 25$ sec., approximatively, the first loss of detachment occurs when the power at the separatrix P_{sep} exceeds the reference value. In view of the simplicity of the divertor model – which is a stationary model [16], thus unable to describe the relevant divertor time scales – the loss of detachment manifests itself which such "spikes" in the target temperature (second panel), and the Ar concentration is adjusted accordingly, this leading to the violently oscillatory behavior, clearly unphysical but still representing an acceptable approximation to indicate that detachment has been lost.

During the loss of detachment, the W erosion from the target increases (third panel). This requires the intervention of about 25 MW of NBI to maintain the fusion power at the desired level, as the tungsten migrates towards the main plasma and starts to radiate. In parallel (third panel), also the core radiator Xe is included in the system to bring the power at the separatrix down to the target value indicated by the thick red line. Once the detachment is lost again shortly after $t = 300$ sec. (this happening because the Ar concentration drops below the minimum value to maintain detachment), the W influx enhances the core radiation and P_{sep} decreases. The system tries to react back by removing Xe (i.e. stopping the injection in the system while maintaining the pumping) and increasing NBI power, but this time it is impossible to prevent the fusion power to deviate from the reference value for some tens of seconds.

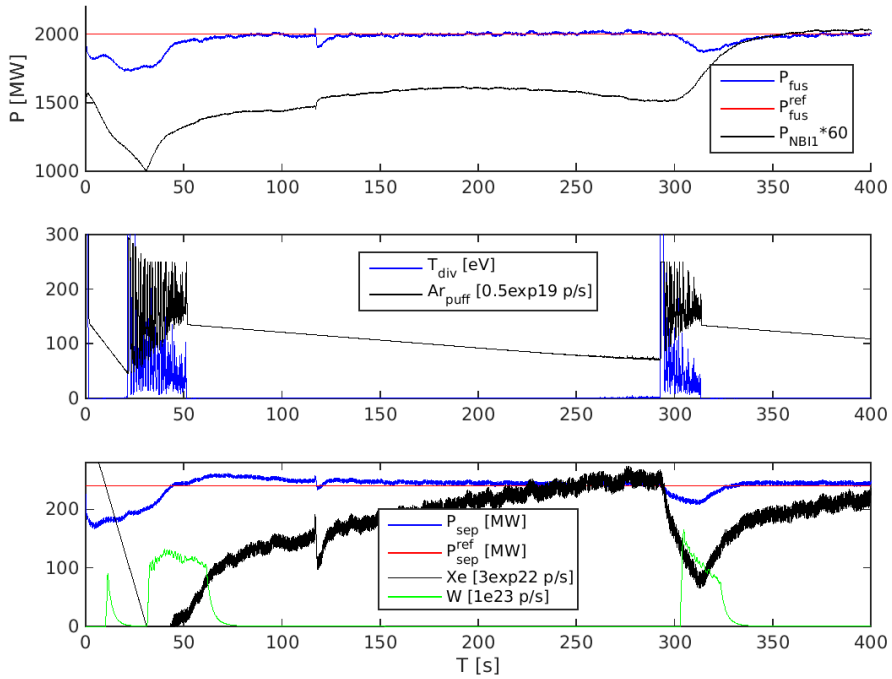

***Figure 3**. Example of simultaneous fusion power and divertor detachment contro with ASTRA/Simulink. In the central plot, the Ar puff increases when the divertor detachment is lost. Loss of detachment causes an increase of W erosion at the plate (bottom), which requires the intervention of NB to maintain the fusion power at the required level of 2 GW (top) to contrast the increased impurity influx. The coupling between ASTRA and the 0D divertor model is described in [16,17].*

In this second case, an accurate representation of the relevant timescale is still missing – as mentioned, reattachment is not expected to happen so fast. As previously mentioned, the development of this tool is currently ongoing, both with the purpose of improving the accuracy of the implemented physics models (as for example the criterion for the sawteeth stabilization – see next section) and also to add other, at present not considered diagnostics and actuators – for example by including plasma position control in order to determine the overall power requirements for a safe reactor operation.

3. Sawteeth (ST) control

Although the presence of ST might also possess some beneficial aspects, for example the increase of He flushing from the centre of the plasma, an uncontrolled crash is very likely to trigger Neoclassical Tearing Modes (NTMs), which in turn are risky in terms of initiating chains of events eventually leading to disruptions. The presence of a large, stabilizing fast particle population – namely the fusion born alphas – is expected to significantly increase the ST period, which implies in parallel a large amplitude ST crash. Preliminary estimates carried out following the empirical method proposed in [18] – see Fig.4 - show that, in DEMO, an acceptable ST period (normalized to the resistive diffusion time) to reduce the risk of NTM would be about 0.02, whereas the natural period is a factor 5-10 larger.

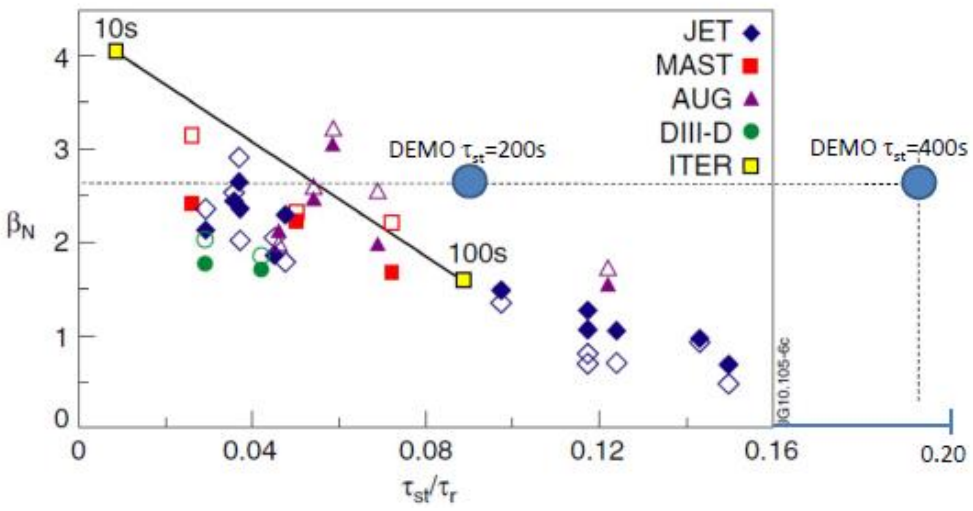

***Figure 4**. Figure adapted from Ref [18]. The experimental points identify the minimum β_N for the onset of NTM after a ST crash as a function of the ST period (expressed in plasma resistive time τ_r units). For the DEMO target value of β_N, the required ST period should then be lower than ~0.02 τ_r, whereas the estimated natural period is a factor 5-10 larger, according to different estimates.*

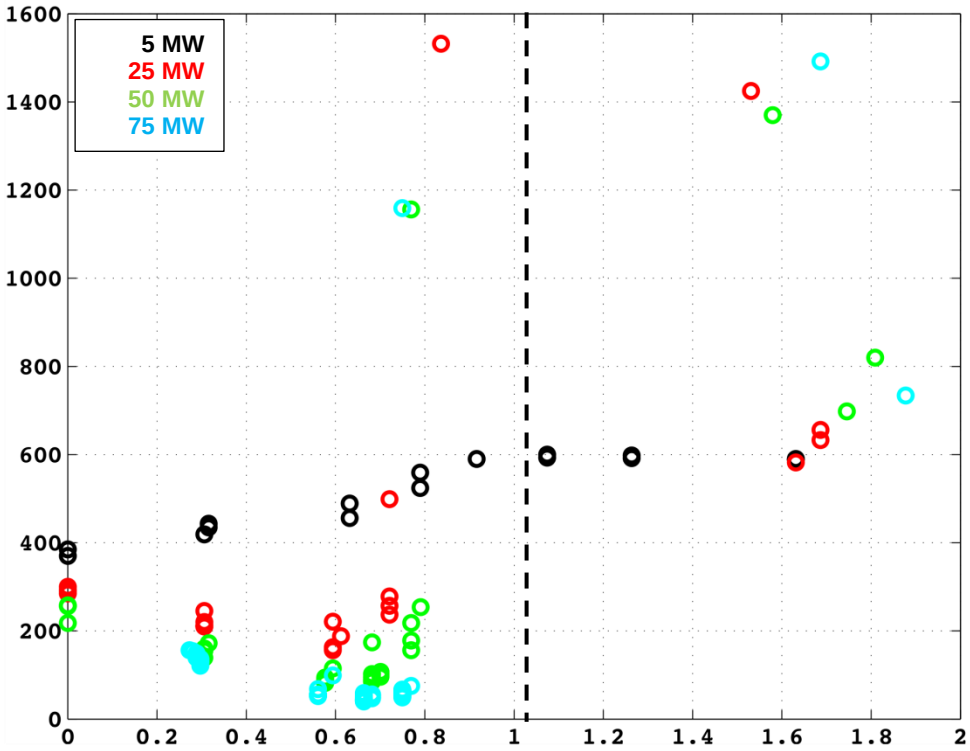

***Figure 5**. Resulting ST period [sec] vs. position of the EC injection, normalized to the inversion radius coordinate. The EC power is identified by the color scale of the symbols. The vertical dashed line identify the q = 1 surface.*

It is therefore to be expected that a ST control strategy based on the destabilization of the mode until the required frequency (and amplitude) is obtained would be particularly demanding in terms of auxiliary heating. For this reason, it is currently assumed for DEMO to pursue a stabilization of the ST rather than a destabilization. In this way, a ST crash under controlled conditions can occur when the EC stabilizing the mode is turned off. In parallel, a pre-emption of the NTMs is undertaken (see a more detailed description of this method in [19]). In Fig. 5, simulations carried out with ASTRA show that this strategy can indeed allow a reduction in the required H&CD power up to a factor 3 compared to the destabilization approach. In these simulations, the stability of the ST is modelled by employing the well-known critical shear criterion proposed by Porcelli et al. [20]. Currently, the ST control power requirement for the H&CD engineering group is set to 30 MW. Alternative approaches, employing for example the IC, or even extending the temporal duration of the NTM pre-emption phase to the whole discharge and avoid any active control of the ST, are also considered.

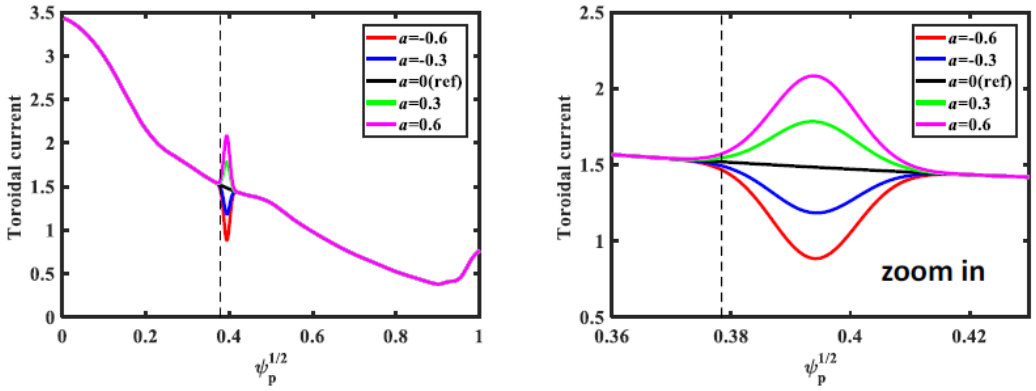

***Figure 6**. MARS-F investigation of the ideal internal kink stability for the DEMO 1 2018 equilibrium in presence of Gaussian-shaped current perturbations in the vicinity of the q = 1 surface for different amplitudes of the perturbation (indicated by the parameter α.in the figures).*

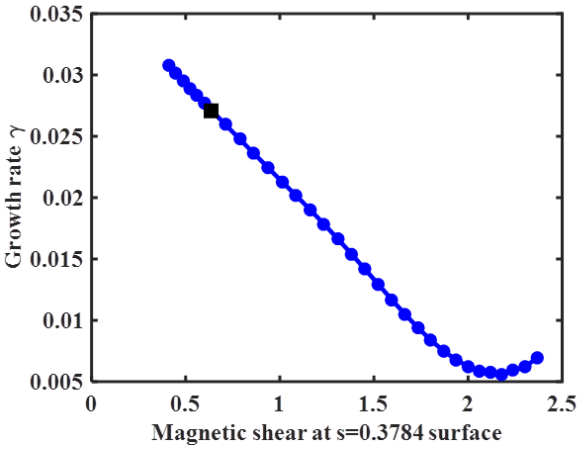

***Figure 7**. Growth rate (normalised to the toroidal Alfvén frequency) of the ideal internal kink as a function of the magnetic shear at the radial location corresponding to the unperturbed q = 1 surface (identified by the flux-surface coordinate s = 0.3784 in MARS-F units). The black square identifies the unperturbed equilibrium (i.e. $\alpha = 0$). The calculation has been performed by keeping the total plasma current constant – this causing a small movement of the q = 1 surface among various cases. At lower growth rates (i.e. below 0.01), the ideal MHD equations are no longer quantitatively valid as additional layer effects –not considered here - become important.*

In parallel, a deeper understanding and more detailed modelling of the ST physics in relevant DEMO conditions is undertaken. A preliminary investigation with the linear MHD code MARS-F [21] has been carried out, addressing the stability of the ideal internal kink, which is prodromal to the ST, in presence of a Gaussian perturbation to the toroidal current profile -a local reduction of toroidal current increases the magnetic shear near the q=1 surface, and vice versa a local increase. Results are summarized in Fig. 6 and 7. As expected from analytic theory, an increasing magnetic shear tends to stabilize the ideal internal kink mode. It is planned for the near future to proceed in this investigation employing the extension MARS-K [22], which will allow the inclusion of stabilizing drift kinetic effects from thermal and energetic particles, as well as more detailed layer effects, like finite Larmor radius (FLR) effects, plasma resistivity, etc. Quantitative data obtained from toroidal computations by MARS-F/K can eventually be incorporated into the Porcelli model mentioned above to investigate the ST behavior, with the long term goal of achieving a more precise determination of the power necessary to the ST control.

4. Integrated core/pedestal predictive modelling

Extensive predictive pedestal modelling using the EPED1 model of EU-DEMO around its operational point [23] identified several parameters that can affect the pedestal height. One of the key parameters was β_p that affects the Shafranov-shift that, in turn, improves the pedestal stability leading to increased predictions for the pedestal top pressure in high β_p plasmas. However, the achieved β_p in a given plasma conditions depends strongly on the pedestal height itself, as it sets the boundary condition for the core transport. Therefore, the coupled core-pedestal model has to be solved self-consistently with a core transport model and auxiliary heating as input (heating from fusion reactions is calculated self-consistently). A simple stiff core transport model has been employed for this investigation, where the heat diffusivity is small up to a critical temperature gradient and then increases rapidly. The critical temperature gradient for this transition to take place, namely $R/L_{T,crit} = 5$, has been taken from JET experiments [24] and gyrokinetic simulations [25,26].

Figure 8 on the left shows the result of the self-consistent simulation where the density and the auxiliary heating power have been varied around the DEMO1 Physics 2018 parameters. As expected, the predicted pedestal temperature increases with power. However, the self-consistently calculated fusion gain decreases rapidly as the heating power is increased. The resulting temperature profile with the actual DEMO 1 values ($P = 50$ MW and $n_{e,ped} = 6.7\ 10^{19}$ m^{-3}) has been observed to agree very well with the ASTRA simulation results shown in Sec 1, in spite of the simplicity of the model. The predicted fusion gain is found to be relatively insensitive to the choice of density.

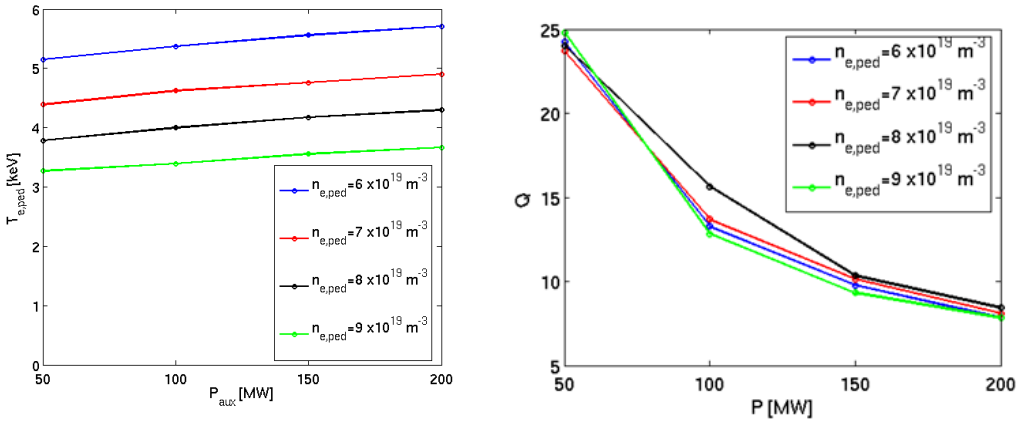

***Figure 8**. The self-consistently calculated pedestal temperature (left) and the total fusion gain (right) as a function of the auxiliary heating power and density using DEMO1 Physics 2018.*

It has to be stressed that the points shown in Fig. 8 have to be understood as different flat-top equilibria, and not as a dynamic series – i.e. no hysteresis on the pedestal top by reduction of the auxiliary power is considered.

5. SOLPS simulations

The foreseen steady-state DEMO divertor operation is being investigated by means of the code SOLPS, using a mixture of Ar and Xe seeded impurities. In particular, Xe is intended to radiate from the core in order to lower the power crossing the separatrix as much as possible (i.e. slightly above the L-H threshold power) to ease the attainment of divertor detachment, whereas Ar, on the contrary, radiates the power in the divertor region so to trigger detachment. In terms of upstream conditions, the parameter space explored so far covers a P_{sep} range extending from 150 to 240 MW, with a fixed power level of 45 MW to electrons and the rest given to ions (other combinations: balanced power and power preferentially given to electrons are currently being analyzed). In all the most recent cases, an upstream density of 2e19 m^{-3}, i.e. below 0.45n_{GW}, in accordance with recent publications identifying such value as an empirical stability limit for the plasma discharge [27], has been employed. In Fig.9, a power scan aiming at determining the minimum required Ar injection for detachment is shown. In these cases, Xe was puffed at a constant rate of 2e10 s^{-1}. Instead, the minimum Ar injection required for detachment was found to vary between 2.5e20 s^{-1} (at P_{sep}=150 MW) and 4.0e21 s^{-1} (at P_{sep} = 240 MW). This is a very strong dependence which seems to be motivated by the need to drive detachment along the complete target (as opposed, for example, just at the strike point). Possibly, simulations assuming a higher fraction of power to the electrons might exhibit a less strong variation of the impurity seeding to reach detachment, as impurity radiation primarily cools down electrons. Fig.9 shows the temperature and heat flux profile along the divertor plate for different cases, varying from deeply attached to detached. Currently, a proxy for detachment is adopted by ensuring the electron temperature to fall below 5 eV and the peak power load on the target (excluding radiation but retaining surface recombination) to be below 10 MW/m^2. All cases run so far assume fluid neutrals, avoiding the time-consuming Monte Carlo transport code EIRENE. A further CPU-saving strategy is the systematic adoption of an aggressive charge states bundling scheme for non-hydrogenic ions [28], which limits to three the number of effective charge states to be followed per each impurity.

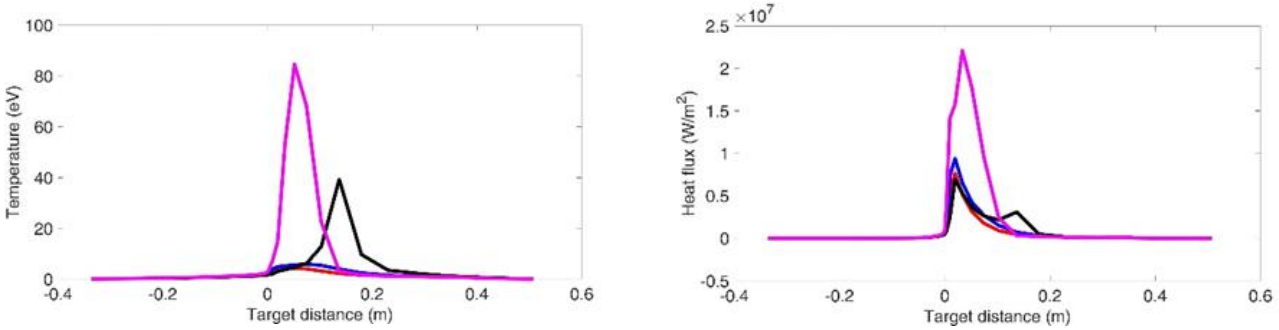

***Figure 9**. SOLPS calculations: temperature (left) and heat flux (right) profiles along the outer target for the SOLPS cases mentioned in the main text. The deepest attached case has P_{sep} = 150 MW and Ar puff 3x10^{20} s^{-1}, the extremely attached case has P_{sep} = 200 MW and Ar puff 4x10^{21} s^{-1}, other cases have intermediate values.The value 0 on the x axis identifies the strike point on the plate.*

More detailed simulations (including kinetic neutrals and following individually each impurity charge state) are ongoing. During 2018, some of the available SOLPS cases have been provided for the development of synthetic diagnostics for the divertor detachment and in support of the design of the pumping system, having included in the dedicated cases for the latter purpose also an He flux of 7.3e20 s^{-1} from the core, corresponding to the 2 GW DEMO fusion power generation. The status of these activities is discussed in section 6 and 7.

Goal for the 2019 activities is to establish a series of reference SOLPS case which have then to be employed also for the engineering activities, at least until the pre-conceptual gate review of the EU-DEMO project planned for 2020 [29].

6. Synthetic diagnostics development

As already recognized in the very beginning of the related investigation [7,8], and as previously mentioned, the DEMO divertor has to be operated in a detached divertor condition, as the heat flux in attached conditions is foreseen to be higher than the technological limit of 10 MW/m^2 by a factor up to 10 in the most severe cases. Figure 10 shows the results obtained with the thermo-hydraulic code RACLETTE [30], where the heat flux on the divertor plate is increased at $t = 0$ from 0 to 40 and 70 MW/m^2, respectively and as a consequence, if no other countermeasures are taken, the coolant reaches the critical heat flux (CHF), and thus the burn out in both cases within two seconds.

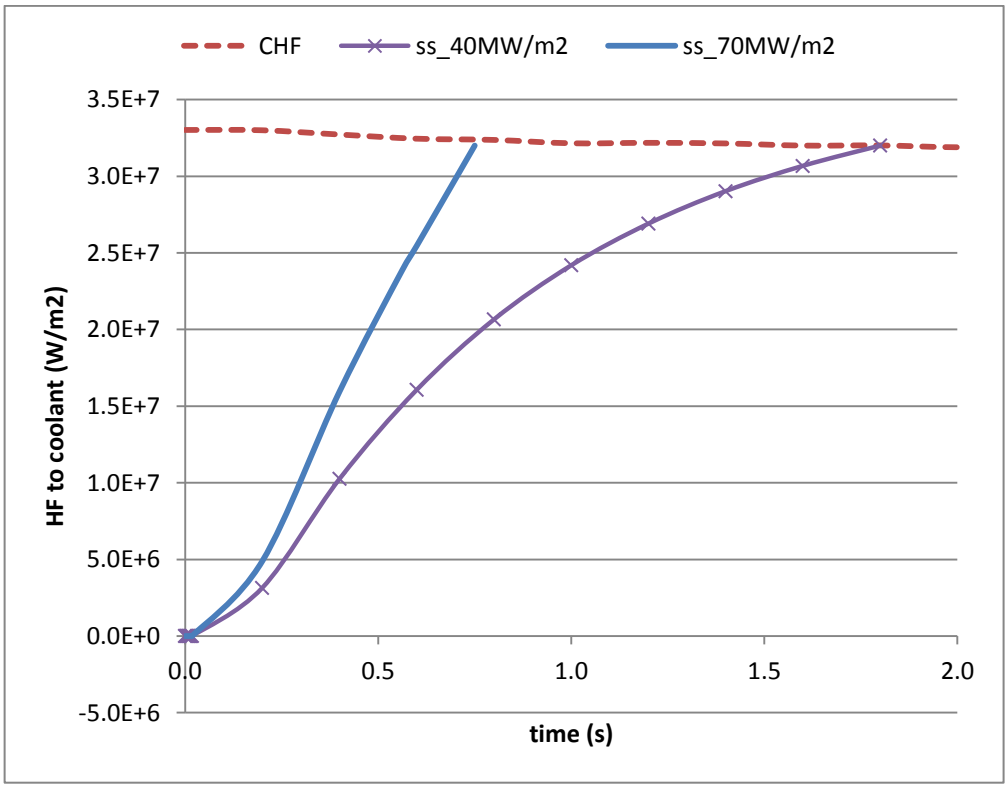

***Figure 10**. Heat flux to the coolant as a function of time in case of an incidental divertor re-attachment At t=0, the incoming heat flux is increased to 40 and 70 MW/m^2, which are values compatible with attached divertor operation.*

Note that these RACLETTE simulations are starting from zero heat flux to the coolant at $t = 0$. In reality, the coolant is already heated when a loss of detachment occurs, thus the process shown here will probably be even faster. As the consequences are so rapid and severe, it is clear that DEMO should be designed to be able:

1. To detect the occurrence of a loss of detachment before the heat flux at the divertor target reaches a dangerous value and

2. To ensure the integrity of the divertor for a sufficiently long time to recover the discharge or to rapidly terminate the plasma in case the detachment cannot be maintained by the dedicated actuators.

For the second point, the actual concept foresees the use of divertor sweeping, which will however not be analysed in the present publication (the interested reader is referred for example to [31,32]). Instead, the first point is the matter of discussion of the present section.

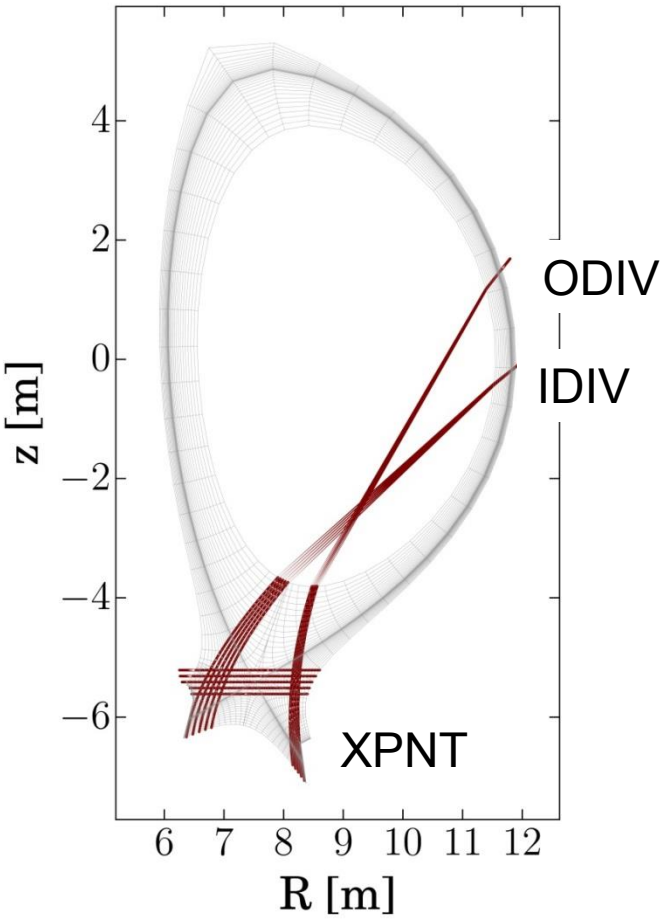

***Figure 11**. Example of lines of sight for the divertor detachment diagnostic. Due to the toroidally inclined sightlines the traces look curved in this 2 plot although in 3D they are straight.ODIV = outer divertor target plate, IDIV = inner divertor target plate, XPNT = X-point*

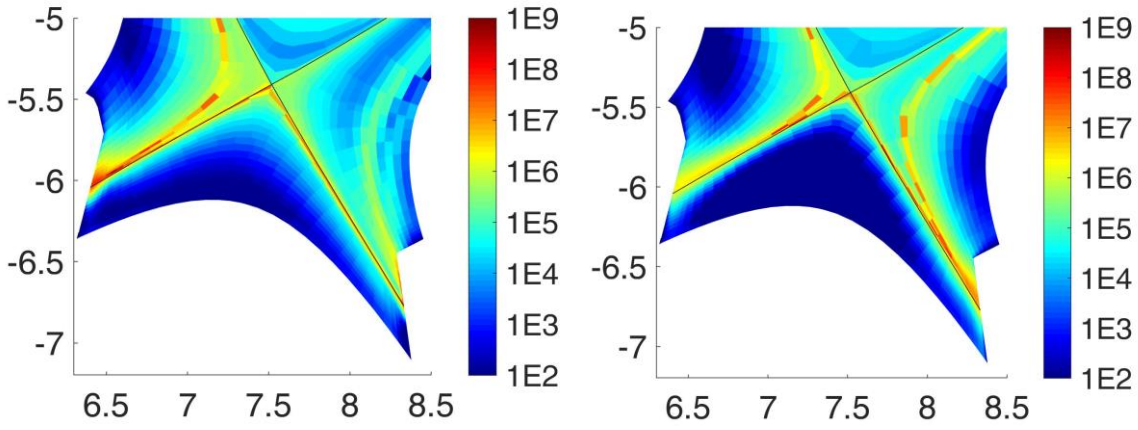

***Figure 12**. Radiation density (W/m^3) in a barely detached case (left - with pressure ratio upstream to target close to one) and in a more strongly detached case (right, with pressure ratio ~4) calculated with SOLPS.*

In present machines, the control of the partially detached regime has been obtained by means of impurity or deuterium seeding [33,34]. Possible control signals employed in current machines include: divertor plate thermoelectric currents [33], integrated radiation provided by bolometry [35], divertor heat flux measured by thermocouples [36], and electron temperature in front of the target from Thomson scattering [34]. However, all these methods do not offer information on spatial displacement of the detachment front, which is an important piece of information not only to guarantee the start of divertor sweeping with sufficient advance, but also to avoid the development of a strong X-point (MARFE-like) radiator within the confined region, as it can degrade confinement and possibly lead to disruptions [37,38].

For these reasons, the feasibility of a detachment control based on visible and UV spectroscopy is going to be investigated. Spectroscopic measurements in different regions of the divertor have been largely used to monitor the status of the detachment given their relatively easy implementation (for a review see [39]). More recently, the ratio of emission lines of nitrogen from

different and equal ionization stages could be used to characterized the detachment evolution [40,41]. Possibly, such method is extensible to other impurities, e.g. Ar. On the same line, the ratio of Balmer-lines has been employed to measure the plasma recombination fraction along the outer divertor leg [42]. Based on these methods, a control signal for the divertor detachment with spectroscopic measurements might be possible.

With the purpose of having an overview of the detachment evolution, the divertor legs and the X-point area need to be diagnosed. Based on the DEMO equilibrium and the vessel design, a first draft of possible lines of sight (LOSs) has been developed (Fig.11). The LOSs have been implemented as synthetic diagnostic in the SOLPS simulation described in the previous section, and synthetic spectra will be calculated as soon as kinetic simulations, i.e. including all the impurity ionization stages, will be ready. A detailed comparison of simulations at different detachment levels is foreseen, with the purpose of investigating the feasibility of this diagnostic concept for a DEMO operation.

Figure 12 shows an example of different radiation distribution in two SOLPS cases when going from attached to detached divertor.

7. Dimensioning of the pumping system

The amount of helium ash which has to be removed by the torus pumping system is determined by the fusion power level. At the expected 2 GW target, the He generation rate corresponds to roughly 10^{21} atoms per second. Although this He flux only represents a small fraction of the total exhausted gas (mainly D, T and impurities) which are passing through the divertor openings and through the port duct and into the pump inlets, it determines a concise requirement for the pumping performance of this coupled system: plasma – divertor – sub-divertor and port duct volume – in-port vacuum pump. The lower limit is defined by the maximum allowed core plasma fuel dilution due to He, which strongly depends on the He backflow from the divertor area. To verify this interface requirement, the feasibility of particle exhaust in DEMO shall be investigated in the near future with flow simulations using the engineering code ITERVAC, employing SOLPS profiles at the target as input. The aim is to quickly compute many designs while satisfying the aforesaid requirement enabling plasma operation.

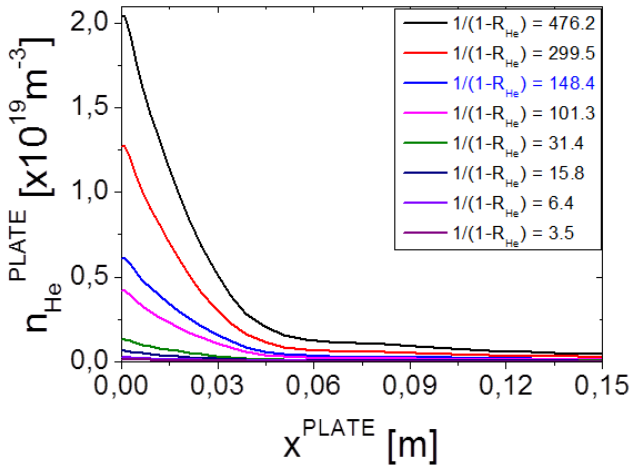

***Figure 13**. COREDIV results: He profile on the target plate for different values of the He recycling coefficient R_{He}.*

In parallel to the SOLPS calculations, He concentration has been investigated as a function of the recycling coefficient of He with the coupled core/SOL code COREDIV [43]. Results are given in Fig.13. Both SOLPS and COREDIV predict a He concentration of the order of >10^{19} He atoms/m^3 at the target, which in view of the foreseen He generation sets the requirement for the pumping system to several hundreds of m^3 per second.

For 2019, a dedicated analysis of He transport coefficients in the SOL, which finally determine the He concentration at the target plate for a given He separatrix density, is foreseen. This will provide interesting pieces of information for the modelling activites on this quite fundamental aspect of the machine design.

8. Ramp-up and down

Both ramp-up and down are crucial phases for DEMO, which have to be performed by minimizing the risk of damaging the machine. This means in particular:

- Ensure the controllability of the plasma column during the ramps, which means especially avoid too large and quick transients in I_p, β_p and l_i, which cannot be followed by the magnetic control system – this implies, for example, exiting the H-mode as late as possible during ramp-down.

- Ensure that the load on the divertor plate never exceeds the technological limit it has been designed for. This might be particularly critical during ramp-up, if for example the H-mode is entered at low density where no detachment would be achievable.

At the same time, an accurate description of the ramp phases is of particular relevance for determining the requirements for the H&CD systems, and also of the poloidal field coils power supply requirements. It has in fact been acknowledged that these phases in DEMO will be particularly demanding in terms of auxiliary power need, in view of the large size of the device (an accurate evaluation is currently ongoing).

Trajectories of the ramps in DEMO have been explored during 2018 with the code RAPTOR [44], which during 2017 has been calibrated to reproduce real, experimental discharges in JET and TCV. Figure 14 shows the time evolution of the plasma internal inductance $li3$ for two different current ramp rates, namely 100 kA/sec (scn1) and 80 kA/sec (scn2).

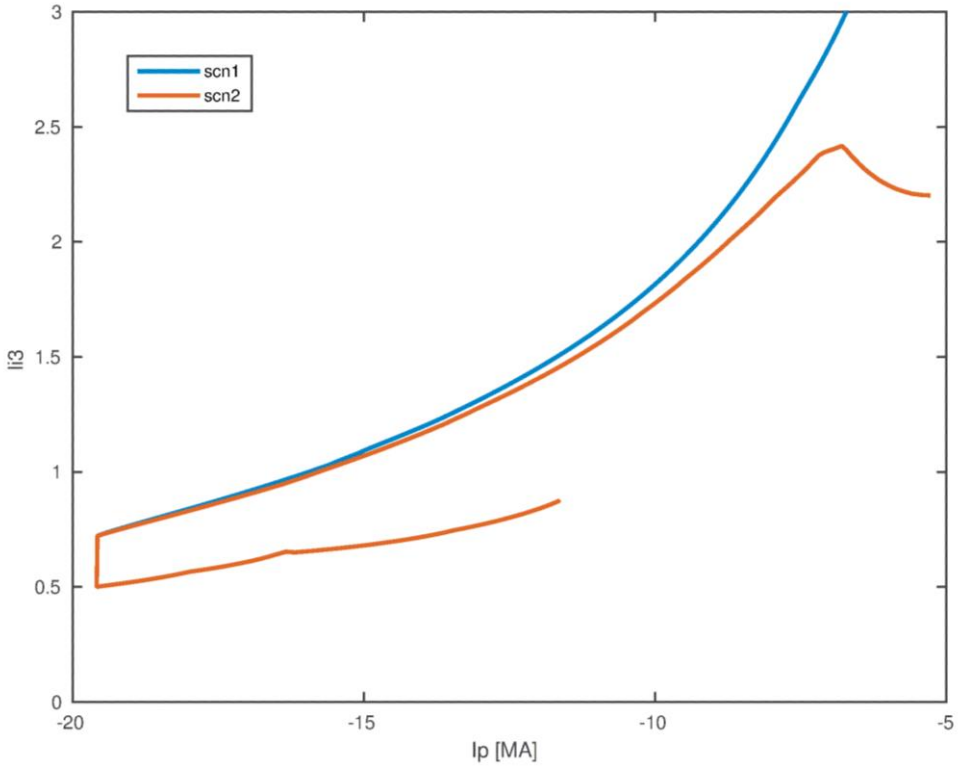

***Figure 14**. Evolution of the internal inductance $li3$ as a function of the plasma current value for two different current ramp rates, namely 100 kA/sec (scn1) and 80 kA/sec (scn2). These curves have been obtained with RAPTOR.*

In the meanwhile, magnetic equilibrium investigations assuming a linear evolution of I_p, β_p and l_i to check the adequacy of the available coil system by the calculation of sequences of free-boundary equilibria have been with the code CREATE [45]. These simulations (which are shown in Fig.15) neglect the self-consistent evolution of the kinetic plasma quantities, as well as the presence of noise in the diagnostics. Both ramp up and ramp down are carried out in the simulation at $dI_p/dt = 100$ kA/s, which is identified as the quickest rate at which the magnetic control is still feasible, up to 19.6 MA (which was the flat-top value of the plasma current in a previous baseline, but the main conclusion are still considered valid).

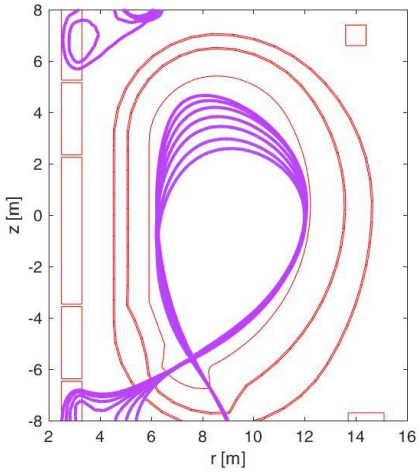

***Figure 15**. Evolution of the magnetic equilibrium for ramp-up and down, assumed at this stage to be simmetric. The present calculation assumes a constant current ramp rate of 100 kA/s. No self-consistent evoultion of the plasma β_p and l_is included at this stage.*

At present, only the diverted phases of the ramps – which are entered (or left) at approximatively one third of the target plasma current – are considered. Also, an obvious consequence of such assumptions is that the ramp-up and down have the same shape sequence, only at reversed order – although it is most probably going not to be the case once further requirements will be implemented.

Plan for the prosecution of the work is to aim at a consistent evolution of the plasma profiles and of the magnetic shapes by coupling the plasma transport codes with magnetic modelling codes, with the purpose of identifying the best trajectories in terms of the above elucidated criteria. An important aspect which is intended to be analyzed is the role of seeded impurities, namely Xe and Ar, as a balance between the need of preserving the divertor compatibility and, at the same time, avoiding the occurrence of radiative instabilities, has to be found and described.

9. Edge Localised Modes (ELMs)

A simple estimate performed by means of the scaling recently suggested in [46] indicates that, in DEMO, a natural type I Edge Localised Mode (ELM) releasing 10% of the pedestal energy will deposit on the target plate the equivalent of ≈ 10 MJ of energy, this happening in around one millisecond. Simulations performed with the code RACLETTE [30] have shown that even a single ELM event of this kind in DEMO will be sufficient to cause melting on the surface of the target plate W coating, and also a few tens of these events will be able to ablate one half of the W layer.

This occurrence poses a serious question mark on all the active control methods for ELM mitigation or suppression, because a reliability of 100% would be then necessary, this engineering target clearly being impossible to meet (even disregarding other drawbacks all active ELM mitigation or suppression techniques have on the plasma performance). For this reason, a plasma scenario which is naturally ELM-free, as for example the QH-mode [12], the I-mode [13], or even a negative triangularity machine [47,48] would be extremely beneficial for the design of a machine like DEMO, whose mission includes quite challenging availability requirements – to a much higher extent than for example ITER.

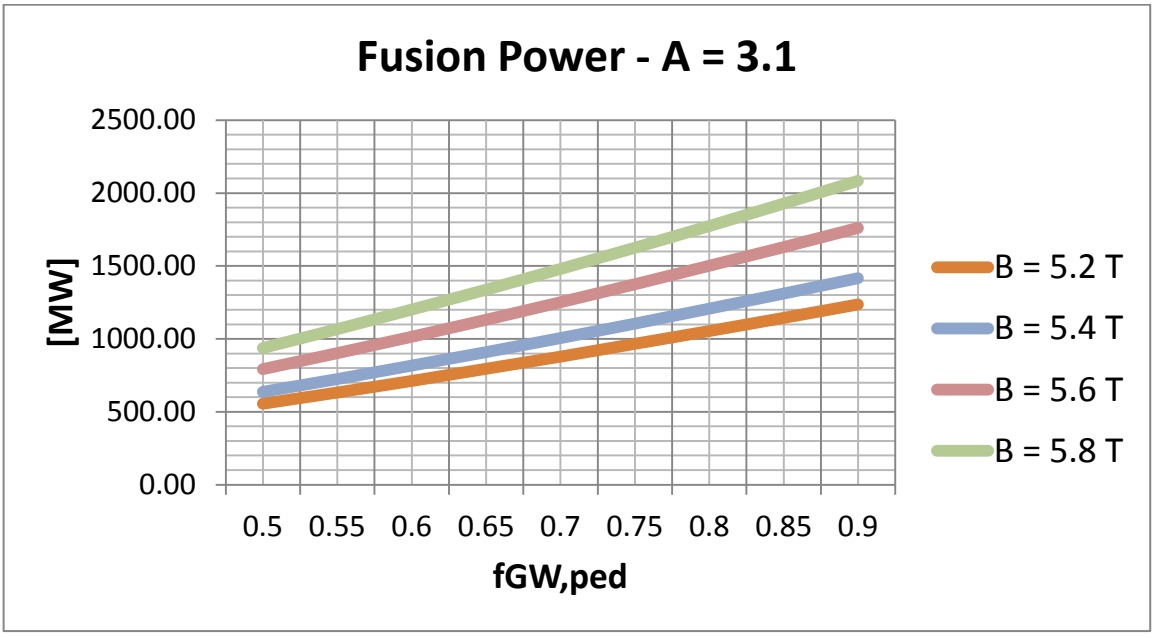

***Figure 16**. Fusion power as a function of the pedestal top density (expressed as a function of Greenwald density). A constant pedestal top pressure – derived with the EPED scaling in [17] – is assumed (thus, the pedestal top temperature increases once the density is decreased). The value of the fusion power has been derived by employing the scaling proposed in [49].*

For the time being, only QH-mode and I-mode are considered as possible candidates for the DEMO baseline. The negative triangularity configuration is still investigated, but in view of the large modifications required on the design of the machine it is at the moment not part of the baseline.

Both QH-mode and I-mode have however a number of features which have to be carefully considered when extrapolated to a reactor device – on top of the low amount of experimental experience available in comparison to the ELMy H-mode. In particular, the main concerns linked to the adoption of the QH mode in a DEMO machine are:

- Difficult accessibility: a high rotational shear in the edge seems to be the main ingredient to access the QH-mode. It is however unclear how this rotational shear requirement translates to a DEMO reactor scale, and also how to reliably obtain it (tangential NBI and also RMP coils [50] are possible candidates for this purpose, but both might exhibit difficulties in integration, especially if a large rotation be needed. There may also be an impact on the allowable toroidal magnetic ripple.)

- Never observed at high density: this might be due to the fact that current machines are not able to operate at high densityand low collisionality at the same time, thus this might extrapolate favourably to DEMO. However, this nowadays prevents the community from exploring some extremely important experimental situations, as for example a QH-mode in presence of detached divertor.

The main concerns towards an I-mode reactor are:

- Absence of density pedestal: in contrast to QH-mode, where there is some indication that the density can be recovered at DEMO scales, the absence of a density pedestal density might not be compensated via extrapolation to a reactor size. In Fig.16, a preliminary investigation carried out with a parameter scaling, in turn derived by a database of ASTRA/TGLF DEMO related cases for different boundary condition at the pedestal top [48], is shown. The figure shows that, if the magnetic field can be held at around 6 T, 1.5 GW fusion would be achievable at I-mode-like density level (~ 0.65 f_{GW}) [51]. Otherwise, the reduction in fusion power might be incompatible with the DEMO mission.

- Larger threshold power than H-mode: the scaling for the LI transition power proposed by Hubbard et al., [52] indicates that the I-mode threshold has a lower dependency on the magnetic field than the LH threshold. However, at DEMO 1 parameters, one observes that still $P_{LI} > P_{LH}$. This is clearly going to exacerbate the problem of reaching divertor detachment (also, as for QH-mode, no experimental observation of detached I-mode plasmas is to our knowledge available). Furthermore, although ELM-free, the I-mode exhibits power "bursts" on the divertor target [51], whose nature is still under investigation.

It is planned for 2019 to release two ELM-free baselines for physics, one assuming a QH-mode plasma and the other assuming an I-mode plasma. The details of such baseline are currently under discussion inside the PPP&T department.

10. Flexi-DEMO

As mentioned in the introduction, the main alternative concept developed for the plasma scenario in Europe is the is so-called Flexi-DEMO scenario, which has been conceived as the intermediate step between ITER and future fusion power plants in the "stepladder" approach [10]. Flexi-DEMO relies on more advanced scenarios as compared to DEMO 1, with a large fraction of auxiliary current drive and a tailoring of the safety factor profile which aims at maximizing the bootstrap current fraction. Ideally, Flexi-DEMO is a steady-state operating machine, but in order to achieve this goal a confinement time larger than that predicted by the IPB98(y,2) scaling (i.e. an H factor of about 1.25) will be required. This kind of performance, however, cannot be robustly inferred from the current experimental experience on these scenarios, although some fully non-inductive discharges have been experimentally observed [53,54]. Thus, the Flexi-DEMO concept relies on the idea of absorbing all the uncertainties connected with the achievable energy confinement and stability limits of the machine by considering also the possibility to add some additional plasma current by employing a central solenoid, whilst keeping both the fusion power and required auxiliary power at a constant level – this in order to avoid significant repercussions on the balance of plant and on the breeding blanket. This clearly implies that, at lower confinement, no steady-state operation will be any longer possible, thus the discharge becomes pulsed – the length of the pulse depending on how large the inductive current fraction must be to ensure the same power, which in turn depends on how distant the achievable confinement time is from the value required for steady-state operation. From the point of view of scenario integration, the main difficulty of Flexi-DEMO is linked to the constant necessity of a high auxiliary current drive (requiring more than 100 MW launched to the plasma), which must be added on top of the other functions of the H&CD systems. In Table 2, a comparison between the DEMO 1 baseline 2018 and the steady state Flexi-DEMO can be found.

	DEMO Physics 2018	Flexi-DEMO Steady State
R [m]	9.00	8.4
B_0 [T]	5.86	5.8
q_{95}	3.89	4.6
I_p [MA]	17.75	14.61
P_{fus} [MW]	2000	2000
P_{el}	500	355
P_{sep} [MW]	170.4	188.2
P_{aux} [MW]	50	120
$H^*_{rad,corr}$	1.1	1.39
H_{98}	0.98	1.23
$< n > / n_{GW}$	1.2	1.42
$< T >$ [keV]	12.49	14.47
f_{BS}	0.39	0.62
f_{NI}	0.39	1

***Table 2**. Flexi-DEMO steady state relevant machine parameters. Corresponding DEMO 1 2018 data are reported for comparison. Data have been produced with the systems code PROCESS. Here, f_{BS} and f_{NI} indicate the bootstrap current fraction and the non inductive fraction of the plasma current, respectively*

Instead, Fig.17 compares the safety factor profiles of DEMO 1, Flexi-DEMO steady state and Flexi-DEMO pulsed at $H = 1$, calculated with ASTRA.

Note that even at $H = 1$, the safety factor of Flexi-DEMO appears to be everywhere larger than 1. This is of course of great benefit in terms of plasma control strategy, as no ST control would be necessary and, consequently, also the NTM control in absence of ST discharge is becoming much less severe – in steady state, even the $q = 3/2$ surface is absent. However, at higher confinement and thus higher β_N, Flexi-DEMO is expected to be prone to Resistive Wall Modes (RWMs), needing therefore active Resonant Magnetic Perturbation (RMP) control coils, whose performance requirements and integrability in DEMO are currently under investigation.

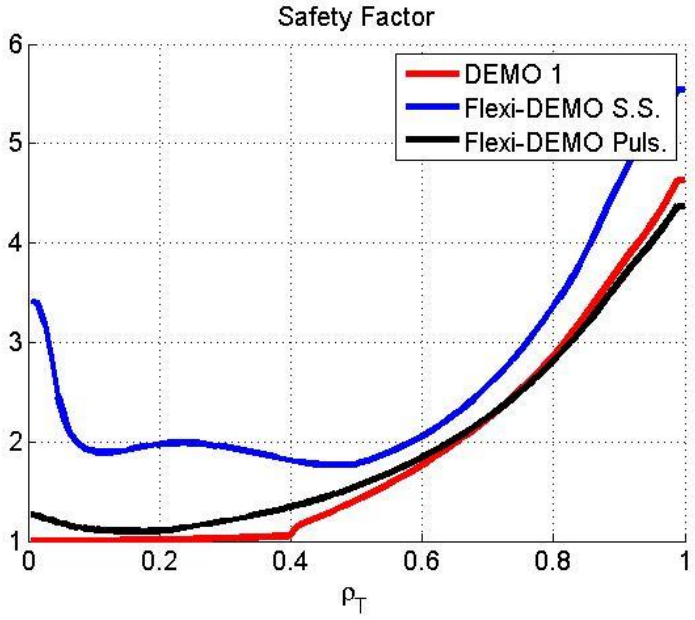

***Figure 17**. Comparison of the safety factor profiles for DEMO 1, Flexi DEMO pulsed at H = 1 and Flexi-DEMO steady state. The value of the safety factor is saturated at q = 1 to mimick the presence of ST activity.*

Most of the currently ongoing investigations about Flexi-DEMO concern a careful assessment of the auxiliary current drive. In fact, in order to maintain a sufficiently large plant electric power output, it is essential that the power required to drive the current remains as low as possible – as one can observe in Table 2 Flexi-DEMO aims at a lower electrical output for the same fusion power as DEMO 1. This means of course maximizing the kA driven by each MW of CD power launched in the plasma.

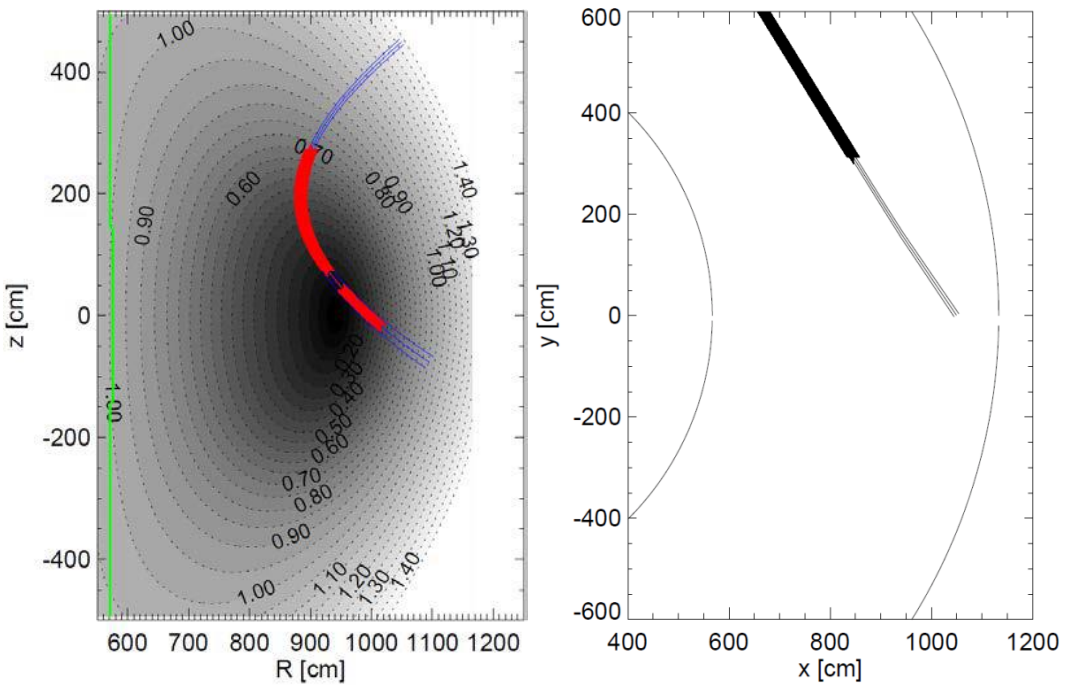

***Figure 18**. Example of ECCD investigation for Flexi-DEMO. Left: TORBEAM modelling of the EC power deposition. Blue lines identify the ray trajectory, the energy deposition area is highlighted in red. The green vertical line highlights the cold electron resonance. Right: top view of the EC beam.*

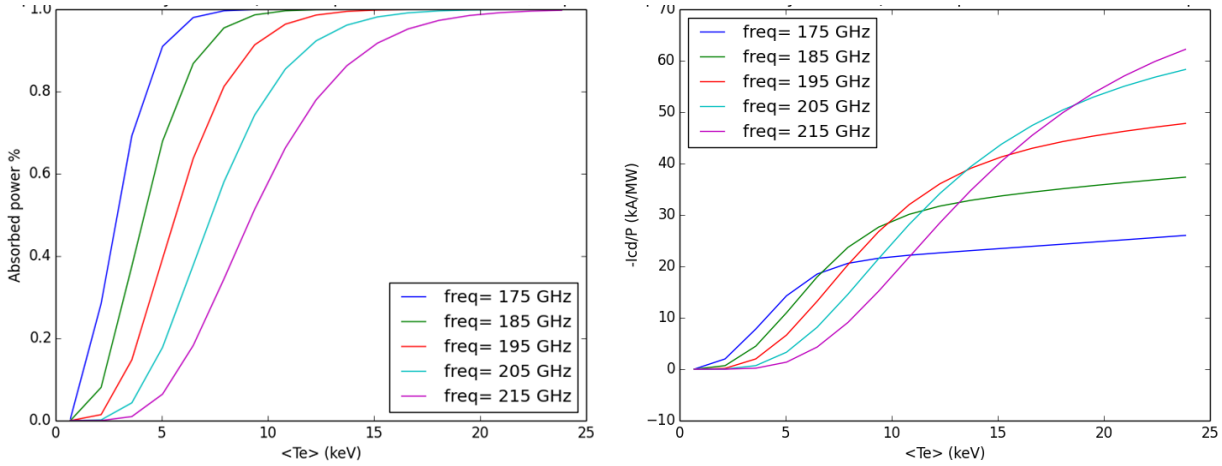

***Figure 19**: GRAY calculations showing the absorbed power fraction (left) and the ECCD coupling efficiency (right) as a function of the line average plasma temperature for different wave frequencies. In this case, the CD is deposited in the plasma centre. The launching angle has been optimised for each of the considered frequencies.*

Investigations on EC current drive are performed with both the code TORBEAM [55,56] and GRAY [57]. Fig. 18 shows an exemplary result about how an EC beam propagates in a Flexi-DEMO plasma, with the absorption region highlighted in red and the cold resonance depicted in green. In this case, an effort has been undertaken about driving the current in an off-axis position, where it is needed to obtain the required safety factor profile. An efficiency of 42 kA/MW for a wave frequency of 240 GHz has been found.

Fig 19 shows the current drive efficiency and the absorbed as a function of the line average plasma temperature and of the launching wave frequency calculated with GRAY. Contrarily to the TORBEAM case, the current is considered to be driven in the plasma centre. The line averaged temperatures is varied from ~1 keV – which is a representative value for the plasma breakdown – up to 24 keV, which is instead the value foreseen by ASTRA for the flat-top phase in case of steady-state discharge. In the initial phases of the plasma discharge (i.e. breakdown and ramp-up), lower frequencies are more efficient in driving the current, whereas for the flat-top very high frequencies become more performing. Thus, a careful identification of the optimal EC frequencies to be installed, and their corresponding power level, will be necessary.

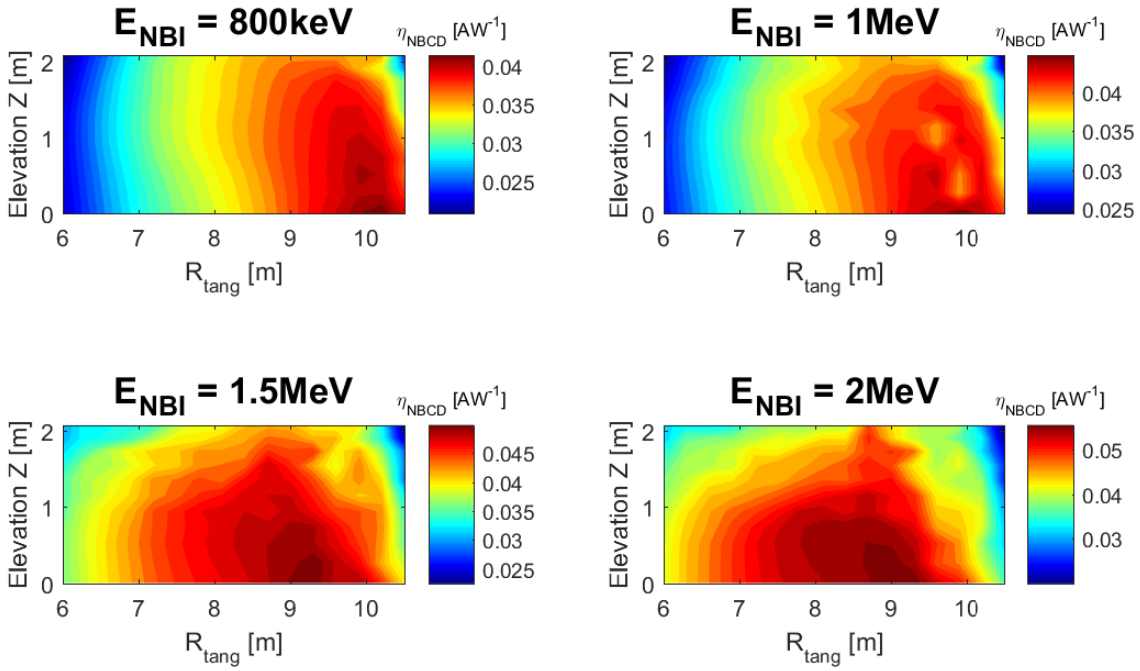

***Figure 20**. NBCD coupling efficiency as a function of the tangential angle and elevation of the beam for two different value of the neutral energy. The investigation has been carried out with the code METIS.*

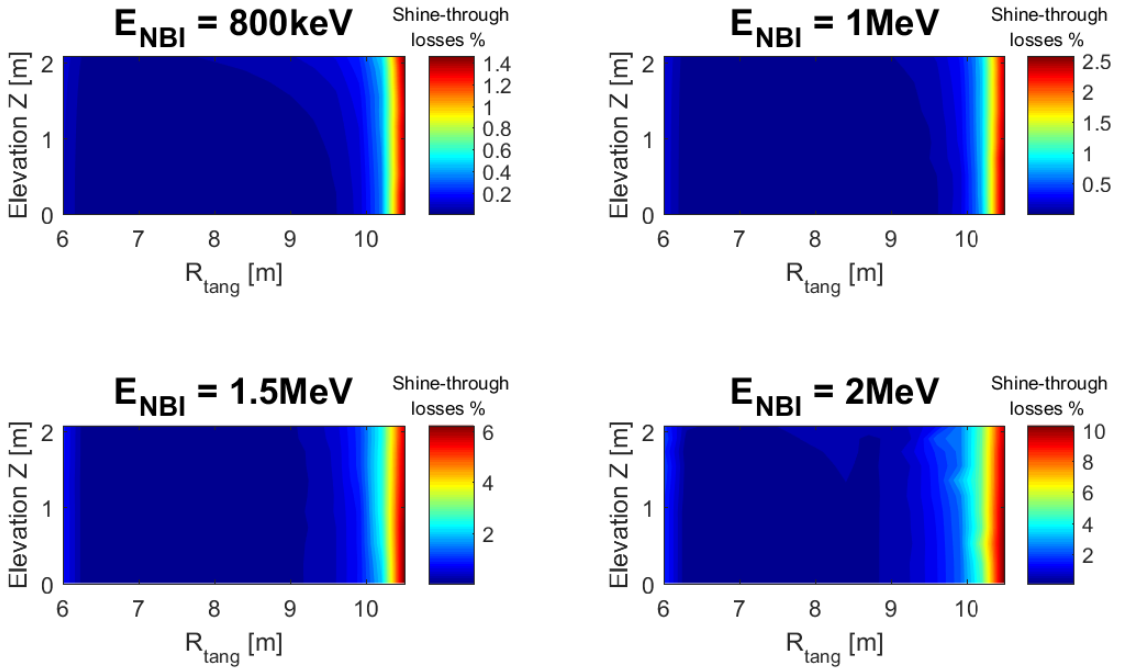

***Figure 21**. NBCD shine-through as a function of the tangential angle and elevation of the beam for two different value of the neutral energy. The investigation has been carried out with the code METIS.*

Fig.20 and 21 show the current drive efficiency and the shine-through for a neutral beam injection (NBI) system for different tangential radii, elevation and energies of the injected particles. The figure has been produced with the code METIS [58], reproducing the equilibrium obtained in the reference ASTRA calculation in Fig. 17 and by assuming the entire required off-axis current to be driven by NB only. For the drive efficiency, values in the range between 40-60 kA/MW are found. From the engineering point of view, it is however difficult to reach beam energies larger than 1 MeV in view of the high necessary voltage. However, it can be seen in Fig.20 that the increase of the energy from 1 to 2 MW does not lead to a spectacular increase of the CD efficiency, but only by about 10%.

Goal of the forthcoming investigations is to find an optimum mix of EC and NB, which is compatible with the H&CD engineering constraints, to maximize the efficiency of the system. This is possibly the most stringent requirement towards the realization of such steady-state reactor concept.

11. Conclusions

Current activities carried out inside EUROfusion PPP&T for the definition of the plasma scenario for the European DEMO have been reviewed in the present paper. The development of the plasma scenario for the DEMO reactor is based on two high level criteria, namely ensuring a sufficiently high fusion power outcome to maintain the net electrical output signicant, and to be able to guarantee the integrity of the plasma facing components for a long operation time. Such requirements have to be met in the framework of an integrated approach to the machine design, as currently carried out in the PPP&T department. This means that a suitable plasma scenario for DEMO, and in general for every next generation electricity producing device, has to be developed by taking into account from the very beginning all the constraints originating from the engineering and technological aspects of the design. In particular, the role of diagnostics, H&CD and fuelling and pumping have been identified as crucial. The activities carried out inside the EU-DEMO project are thus focussing not only towards a deeper understanding of the physics governing DEMO plasmas, but also they are characterised by a strict collaboration with the technological development, in order to rely from the very beginning on solutions which are compatible with an integrated and consistent approach to the machine design.

ACKNOWLEDGEMENTS

This work has been carried out within the framework of the EUROfusion Consortium and has received funding from the Euratom research and training programme 2014-2018 and 2019-2020 under grant agreement No 633053. The views and opinions expressed herein do not necessarily reflect those of the European Commission.

REFERENCES

[1] Romanelli F. et al 2012 A roadmap to the realisation of fusion energy, EFDA Document
[2] Pereverzev G.V., 1991 IPP Report 5/42
[3] Pereverzev G.V. and Yushmanov P.N., 2002 IPP Report 5/98
[4] Fable E. et al., 2013 Plasma Phys. Control. Fusion 55 124028
[5] Kovari M. et al., 2014 Fusion Eng. and Design 89 3054
[6] Kovari M.et al., 2016 Fusion Eng. and Design. 104 9
[7] Wenninger R.et al., 2015 Nucl. Fusion 55 063003
[8] Wenninger R. et al., 2017 Nucl. Fusion 57 046002
[9] Federici G. et al., 2017 Int. Symp. on Fusion Nuclear technology (ISFNT), Kyoto, Japan, to be published
[10] Zohm H. et al., 2017 Nucl. Fusion 57 086002
[11] Janky F. et al., 2017 Fusion Eng. and Design 123, 555
[12] Burrell K. H. et al., 2002 Plasma Phys. Control. Fusion 44, A253
[13] Ryter F. et al., 2017 Nucl. Fusion 57, 016004
[14] Eich Th. et al., 2011 Phys. Rev. Lett. 107 215001
[15] Eich Th. et al., 2013 Nucl. Fusion 53 093031
[16] Siccinio M. et al., 2016 Plasma Phys. Control. Fusion 58, 125011
[17] Siccinio M. et al., 2018 Nucl. Fusion 58, 016032
[18] Chapman I. et al., 2010 Nucl. Fusion. 50 102001
[19] Goodman T. P. et al., 2011 Phys. Rev. Letters 106, 245002
[20] Porcelli F. et al., 1996 Plasma Phys. Control. Fusion 38, 2163.
[21] Liu Y.Q., 2000 Phys. Plasmas 7, 3681
[22] Liu Y.Q. et al., 2008 Phys. Plasmas 15, 112503
[23] Kim S. K. et al., 2018 Nucl. Fusion 58 016036
[24] Mantica P. et al., 2009 Phys. Rev. Lett. 102, 175002
[25] Dimits A. M. et al., 2000 Phys. Plasmas 7, 969
[26] Jenko F., Dorland W. and Hammett G. W., 2001 Phys Plasmas 8, 4096
[27] Eich Th. Et al., 2018 Nucl. Fusion 58, 034001
[28] Bonnin X. and Coster D., 2011 Journal of Nucl. Mat., 415, S488
[29] Federici G. et al., submitted to Nucl. Fusion – IAEA FEC 2018
[30] Raffray A.R. and Federici G., 1997 J. Nucl. Mater. 244, 85
[31] Maviglia F. et al., 2016 Fusion Eng. Des. 109 1067
[32] Siccinio M. et al., submitted to Nucl. Fusion

[33] Kallenbach A. et al., 2015 Nucl. Fusion 55, 053026
[34] Eldon D. et al., 2017 Nucl. Fusion 57, 066039
[35] Goetz J. A et al., 1995 Journal of Nucl. Mat. 220-222, 971
[36] Brunner D. et al., 2017 Nucl. Fusion 57, 086030
[37] Petrie T. W. et al., 1997 Nucl. Fusion 37, 643
[38] Reimold F. et al., 2015 Nucl. Fusion 55, 033004
[39] Leonard A. W., 2018 Plasma Phys. Control. Fusion 60, 044001
[40] Reinke M. L. et al., 2017 Nucl. Mat. and Energy 12, 91
[41] Henderson S. S. et al., 2018 Nucl. Fusion 58, 016047
[42] Verhaegh K. et al., 2017 Nucl. Mat. and Energy 12, 1112
[43] Ivanova-Stanik I. et al., submitted to Fus. Eng. Des.
[44] Felici F. et al., 2011 Nucl. Fusion 51, 083052
[45] Albanese R., Ambrosino R. and Mattei M., 2015 Fus. Eng. Des. 96-97, 664
[46] Eich Th. et al., 2017 Nuclear Materials and Energy 12, 84
[47] Camenen Y. et al., 2017 Nucl. Fusion 57, 086002
[48] Medvedev S. Yu. Et al., 2015 Nucl. Fusion 55, 063013 (2015)
[49] Palermo F. et al., submitted to Plasma Phys. Control. Fusion
[50] Garofalo A. M. et al., 2011 Nucl. Fusion 51, 083018
[51] Happel T. et al., submitted to Nucl. Fusion – IAEA FEC 2018
[52] Hubbard, A. E. et al., 2017 Nucl. Fusion 57. 126039
[53] Bock A. et al., 2017 Nucl. Fusion 57, 126041
[54] Turco F. et al., submitted to Nucl. Fusion – IAEA FEC 2018
[55] Poli E., Peeters A. G. and Pereverzev G. V., 2001 Comp. Phys. Comm. 136, 90
[56] Poli E. et al., 2018 Comp. Phys. Comm. 225, 36
[57] Farina D., 2007 Fus. Sci. Tech. 52, 154
[58] Artaud J. F. et al., 2018 Nucl. Fusion 58, 105001